Monthly Notices of the ROYAL ASTRONOMICAL SOCIETY

MNRAS **518,** L13–L18 (2023) https://doi.org/10.1093/mnrasl/slac125
Advance Access publication 2022 October 16

Intranight optical variability of low-mass active galactic nuclei: a pointer to blazar-like activity

Gopal-Krishna,[1] Krishan Chand ,[2,3]★ Hum Chand ,[4]★ Vibhore Negi ,[2] Sapna Mishra,[5] S. Britzen[6] and P. S. Bisht[7]

[1]*UM-DAE Centre for Excellence in Basic Sciences, Vidyanagari, Mumbai 400098, India*
[2]*Aryabhatta Research Institute of Observational Sciences (ARIES), Manora Peak, Nainital 263002, India*
[3]*Department of Physics, Kumaun University, Nainital 263002, India*
[4]*Department of Physics and Astronomical Science, Central University of Himachal Pradesh (CUHP), Dharamshala 176215, India*
[5]*Inter-University Centre for Astronomy and Astrophysics (IUCAA), Postbag 4, Ganeshkhind, Pune 411007, India*
[6]*Max-Planck-Institut f. Radioastronomie, Auf den Huegel 69, D-53121 Bonn, Germany*
[7]*Department of Physics, Soban Singh Jeena University, Almora 263601, India*

Accepted 2022 October 9. Received 2022 October 3; in original form 2022 September 9

ABSTRACT

This study aims to characterize, for the first time, intranight optical variability (INOV) of low-mass active galactic nuclei (LMAGNs) which host a black hole (BH) of mass $M_{BH} \sim 10^6 M_\odot$, i.e. even less massive than the Galactic centre BH Sgr A∗ and 2–3 orders of magnitude below the supermassive black holes (SMBHs, $M_{BH} \sim 10^8$–$10^9 M_\odot$), which are believed to power quasars. Thus, LMAGNs are a crucial subclass of AGNs filling the wide gap between SMBH and stellar-mass BHs of Galactic X-ray binaries. We have carried out a 36-session campaign of intranight optical monitoring of a well-defined, representative sample of 12 LMAGNs already detected in X-ray and radio bands. This set of LMAGNs is found to exhibit INOV at a level statistically comparable to that observed for blazars ($M_{BH} \gtrsim 10^{8–9}\ M_\odot$) and for the γ-ray-detected Narrow-line Seyfert1 galaxies ($M_{BH} \sim 10^7\ M_\odot$) which, too, are believed to have relativistic jets. This indicates that the blazar-level activity can even be sustained by central engines with BHs near the upper limit for intermediate-mass BHs ($M_{BH} \sim 10^3$–$10^6 M_\odot$).

Key words: galaxies: active – galaxies: jets – galaxies: photometry – quasars: general.

1 INTRODUCTION

Luminous active galactic nuclei (AGNs) of massive galaxies are believed to be powered by accretion on to supermassive black holes (SMBHs) of masses $M_{BH} \gtrsim 10^8 M_\odot$. Powerful non-thermal radio jets are known to be ejected by a significant minority of such SMBH and also by accreting stellar-mass BHs in the galaxy (cf. reviews by Urry & Padovani 1995; Blandford, Meier & Readhead 2019). However, evidence is very sparse about such activity in BHs that fill the huge mass gap between supermassive and stellar-mass BHs, particularly about 'intermediate-mass black holes' (IMBHs) with $M_{BH} \sim 10^3$–$10^6 M_\odot$ (e.g. Greene, Strader & Ho 2020 and references therein; Seepaul, Pacucci & Narayan 2022). Such BHs are thought to exist in moderately massive, or dwarf galaxies (e.g. Kormendy & Ho 2013; Graham 2016). Although essentially no information is presently available about the jet-forming capability of such BHs, work over the past ∼25 yr has found evidence for 'normal' AGN activity occurring in galaxy centres harbouring BHs of masses down to $\sim 10^5 M_\odot$ (Greene et al. 2020), with those having M_{BH} above $\sim 10^{6.5}\ M_\odot$ typically deemed to be normal AGNs (e.g. Qian et al. 2018).

A generic manifestation of AGN activity is flux variability across the spectrum, most conspicuously observed in the tiny subset, called blazars. These include BL Lac objects and flat-spectrum radio quasars, specifically their high-polarization subset, called HPQs. Intensity of blazars is usually dominated by relativistic jets of non-thermal radiation Doppler boosted in our direction. Their observed strong variability is thought to arise from shocks or bulk injection of energetic particles in the jet (e.g. Marscher & Gear 1985; Valtaoja et al. 1992; Spada et al. 2001; Giannios 2010), or, alternatively, due to jet helicity/swings (Camenzind & Krockenberger 1992; Gopal-Krishna & Wiita 1992), or jet precession (e.g. Abraham 2000; Britzen et al. 2018). The rapid (hour/minute-like) flux variability of blazars has been most conspicuously detected at TeV energies, on time-scales as short as a few minutes (Aharonian et al. 2007; Albert et al. 2007), which are much shorter than light-crossing times at a $10^8 M_\odot$ BH's horizon (∼15 min), suggesting that the variability involves small regions of enhanced emission within an outflowing jet (Begelman, Fabian & Rees 2008). Rapid variability has been most extensively documented in the optical band and termed 'intranight optical variability' (INOV, Gopal-Krishna et al. 2003). A likely cause of INOV of blazars, too, is a strong relativistic enhancement of small fluctuations arising through turbulent pockets in the jet (Marscher & Travis 1991; Goyal et al. 2012; Calafut & Wiita 2015). The occurrence of strong INOV of HPQs (blazars which are always radio-loud) and the low-polarization radio quasars (LPRQs) was compared by Goyal et al. (2012), by carrying out sensitive and densely sampled intranight optical monitoring of nine HPQs and 12 LPRQs (both having flat radio spectrum). Remarkably, the HPQ

★ E-mail: krishanchand007.kc@gmail.com (KC); humchand@gmail.com (HC)

subset showed strong INOV (i.e. amplitude $\psi > 4$ per cent) on 11 out of 29 nights, in stark contrast to the LPRQs for which strong INOV was observed on just one out of 44 nights. Evidently, a strong INOV can be an effective tracer of blazar activity in AGNs. Here, it may be mentioned that (low-level) INOV has also been observed in radio-quiet quasars (RQQs) which launch at most feeble jets (e.g. Kellermann et al. 2016). Their INOV may well be associated with (transient) shocks (Chakrabarti & Wiita 1993) and/or 'hot spots' (Mangalam & Wiita 1993) in the accretion disc around the SMBH. However, INOV of RQQs is almost always weak ($\psi < 3$ per cent) and even that is detected in just $\sim$ 10 per cent of the sessions, which is similar to the INOV pattern observed for non-blazar-type jetted AGNs, such as lobe-dominated quasars and even weakly polarized radio core-dominated quasars (Stalin et al. 2004; Goyal et al. 2013; Gopal-Krishna & Wiita 2018).

A related class of AGNs exhibiting strong INOV with a fairly high duty cycle (DC) of $\sim$25 per cent (also, Paliya et al. 2013; Ojha, Chand & Gopal-Krishna 2021) is the tiny, radio-loud minority of Narrow-line Seyfert1 (NLS1) galaxies which have extreme properties similar to blazars, like a flat radio spectrum, high brightness temperature (e.g. Yuan et al. 2008), and *γ-ray* detection, all of which are widely interpreted in terms of a relativistically beamed jet (e.g. Abdo et al. 2009; Foschini 2011; Blandford et al. 2019). This premise is further confirmed by the direct detection of VLBI jets in such sources (e.g. Giroletti et al. 2011). While all this evidence affirms the relativistic jet connection to their strong INOV, an important difference from blazars is that the BHs in radio-loud NLS1 galaxies are estimated to be typically an order-of-magnitude less massive ($\sim 10^7 M_\odot$; e.g. Yuan et al. 2008; Dong et al. 2012; Foschini 2020), estimated through application of the virial method (e.g. Wandel, Peterson & Malkan 1999; Kaspi et al. 2000; Vestergaard & Peterson 2006) which employs full width at half-maximum (FWHM) of the broad-line region (BLR) emission lines and the continuum luminosity measured by single-epoch optical spectroscopy. Thus, powerful relativistic jets do appear to get ejected even by moderately massive BHs, although indications are that the bulk Lorenz factor of such jets is typically smaller with respect to blazar jets (Paliya et al. 2019), an inference also supported by radio observations (Angelakis et al. 2015; Gu et al. 2015; Fuhrmann et al. 2016).

Coming to a further an order-of-magnitude less massive BHs powering low-mass active galactic nuclei (LMAGNs), the question arises if they are at all capable of blazar-like activity? This question is addressed here by determining their INOV properties which, as mentioned above, can be an effective discriminator between blazars and non-blazars. In this first such attempt we have used a representative sample of 12 LMAGNs whose central engines have masses close to $10^6 M_\odot$, i.e. between the lower mass end for normal AGNs and the upper mass end of IMBHs. These LMAGNs are less massive than even the BH Sgr A$*$ located at the nucleus of our galaxy ($M_{BH} \sim 4 \times 10^6 M_\odot$ GRAVITY Collaboration 2018; Witzel et al. 2021), in which a faint non-thermal radio jet has been detected (Yusef-Zadeh et al. 2020). In an extreme event, this highly variable source has shown a factor of 75 change in flux over a 2 h time span, at near-infrared wavelengths where, unlike the optical band, its emission is not masked out by the opacity of the intervening galactic material (see e.g. Do et al. 2019).

2 THE SAMPLE OF LOW-MASS AGNS

Our sample of 12 LMAGNs has been extracted from a well-defined set of 29 such broad-line objects, assembled by Qian et al. (2018), using the criteria of a detected counterpart in X-ray and radio bands, and an M_{BH} in the range $\sim 10^{5.5}$–$10^{6.5} M_\odot$ (These objects were selected by them from Dong et al. 2012 and other literature). Their BH masses had been determined by applying the virial estimator to carefully measured width and luminosity of the broad Hα line in single-epoch spectrum and, according to Qian et al. (2018), the typical uncertainty of these mass estimates is $\sim$0.6 dex. To these 29 LMAGNs we applied a cut in the g-band (SDSS) magnitude, $m_g < 17.0$ [for two sources, J010927.02+354305.00 and J083615.12−262434.16, lacking m_g (SDSS), we used m_V (SIMBAD) together with the transformation equation of Jester et al. 2005]. The shortlisted 13 LMAGNs had one source (J083615.12−262434.16) located too far south for our telescopes, and its exclusion led to our final sample of 12 LMAGNs (Table 1). Their M_{BH} values are tightly clustered around the median of $10^6 M_\odot$, and none exceeds $2 \times 10^6 M_\odot$. As seen from Table 1, all these AGNs have $z \lesssim 0.1$ and a radio-loudness parameter $R_{5\rm GHz} < 10$ ($R_{5\rm GHz}$ is the ratio of radio to optical flux densities, Kellermann et al. 1989). This value is well within the conventional upper limit of $R_{1.4\rm GHz} = 19$ for RQQs, when translated to 1.4 GHz and B band (e.g. Yuan et al. 2008; Komossa 2018). Their 'radio-quiet' classification is also consistent with the radio luminosity limit of 5×10^{29} erg Hz^{-1} at 1.4 GHz specified for RQQs, since such radio luminosities can even arise from star formation in the host galaxy (Kellermann et al. 2016).

3 OBSERVATIONS, DATA REDUCTION, AND ANALYSIS

Three sessions of minimum 3 h duration each were devoted to each of the 12 sources (online Table S2). The monitoring was done in the R band (where the CCD detector used has maximum sensitivity), using the 1.3-m Devasthal Fast Optical Telescope (DFOT; Sagar et al. 2011, 34 sessions) and the 1.04-m Sampurnanand Telescope (ST; Sagar 1999, two sessions), both operated by the Aryabhatta Research Institute of observational sciencES (ARIES), Nainital, India. Details of the observational set-up and procedure can be found in Mishra et al. (2019) and Ojha et al. (2020). A log of the observations, together with data on the comparison stars used here for differential photometry, are provided in the online Table S1.

Pre-processing of the raw images (bias subtraction, flat-fielding, and cosmic ray removal) was done using the standard tasks available in the IMAGE REDUCTION AND ANALYSIS FACILITY (IRAF).[1] The instrumental magnitudes of the target AGNs and the chosen (non-varying) comparison stars in the same CCD frame were determined for each frame, by aperture photometry (Stetson 1987, 1992), using the Dominion Astronomical Observatory Photometry II (DAOPHOT II algorithm). Also, for each frame, we determined the 'point spread function' (PSF) by averaging the FWHMs of the profiles of five bright unsaturated stars within the frame. Median of the PSF values for all the frames in a session gave the 'seeing' (FWHM of the PSF) for the session. Based on prior experience, we took 2×FWHM as the aperture radius for photometry for the session. The estimated INOV parameters for the sample were found to remain essentially unchanged when, as a check, aperture radius was set equal to 3×FWHM. Since our targets are nearby AGNs ($z \lesssim 0.1$), their aperture photometry may have a significant contribution from the underlying host galaxy. It is therefore important that the PSF does not have any systematic drift through the session (see e.g. Cellone, Romero & Combi 2000; Nilsson et al. 2007). This is indeed the case for a large majority of our 36 sessions, as seen from the bottom panel

[1] http://iraf.noao.edu/

Table 1. Basic properties of the sample of 12 X-ray- and radio-detected low-mass AGNs.

Source SDSS name	z	m_g	m_B	M_B	galaxy type	log$M_{\rm BH}$	log($L_b/L_{\rm Edd}$)	Flux at B	Flux at 1.4 GHz	Radio loudness	$P_{1.4\,(\rm GHz)}$
	NED	SDSS			SDSS			(mJy)	(mJy)	$R_{1.4(\rm GHz)}$	(erg s^{-1} Hz^{-1})
(1)	(2)	(3)	(4)	(5)	(6)	(7)	(8)	(9)	(10)	(11)	(12)
J010927.02+354305.00	0.00006[a]	12.27[b]	12.56	−15.60	SA0$^{-(s)\,1}$	5.65	−5.5†	42.85	3.40∗	0.08	7.48×10^{25}
J030417.70+002827.40	0.04443	15.83	17.86	−18.50	Sc^2	6.20	−0.6	0.33	0.62	1.88	2.60×10^{28}
J073106.87+392644.70	0.04832	15.89	19.07	−17.50	Sbc^2	6.00	−0.7	0.11	0.61	5.55	3.10×10^{28}
J082443.29+295923.60	0.02542	15.92	16.32	−18.80	$S0^2_-$	5.70	−0.8∗	1.34	1.67	1.25	2.23×10^{28}
J082433.33+380013.10	0.10316	16.63	16.81	−21.50	Spiral∗	6.10	−0.4	0.86	1.07	1.24	2.70×10^{29}
J085152.63+522833.00	0.06449	16.45	19.16	−18.10	Uncertain∗	5.80	−0.6	0.10	0.92	9.20	8.83×10^{28}
J104504.23+114508.78	0.05480	16.56	16.99	−19.90	Uncertain∗	6.20	−0.8	0.72	0.82	1.14	5.60×10^{28}
J110501.99+594103.70	0.03369	15.15	15.07	−20.70	Spiral∗	5.58	−0.5∗	4.25	5.96†	1.40	1.45×10^{29}
J122548.86+333248.90	0.00106	14.24	10.80	−17.30	SA(s)m0^1	5.56	−2.9†	216.77	1.12	0.01	2.33×10^{25}
J132428.24+044629.70	0.02133	16.09	16.46[c]	−18.51[e]	S0/a^2	5.81	−1.4	1.18	1.79	1.52	2.09×10^{28}
J140040.57−015518.30	0.02505	15.91	17.00	−18.10	compact^3	6.30	−1.4	0.72	1.75	2.43	2.30×10^{28}
J155909.63+350147.50	0.03148	14.61	15.69	−20.00	SB(r)b^1	6.31	−0.2∗	2.40	2.72	1.13	6.15×10^{28}

*Notes.***Col. 2**: '*a*': Wilson et al. (2012); **Col. 3**: m$_g$ from SDSS DR14 (Abolfathi et al. 2018) and the g-mag marked '*b*' is estimated from m_B & m_V (SIMBAD) using the
transformation given by Jester et al. (2005); **Col. 4**: From Véron-Cetty & Véron (2010). The entry marked '*c*' has been estimated from m_u & m_g (SIMBAD) using the
transformation given by Jester et al. (2005); **Col. 5**: M_B taken from Véron-Cetty & Véron (2010). '*e*' Estimated from m_B, using the distance modulus taken from NED;
Col. 6: '∗' SDSS DR14 (Abolfathi et al. 2018), (1): de Vaucouleurs et al. (1991), (2): Nair & Abraham (2010), (3): Zwicky, Sargent & Kowal (1975); **Col. 7**: Taken from Qian et al. (2018);
Col. 8: Eddington ratio, taken from Dong et al. (2012) except for those marked with '∗' and '†', for which the references are Greene & Ho (2007) and Nyland et al. (2012),
respectively; **Col. 9**: Calculated from m_B, following Schmidt & Green (1983); **Col. 10**: Taken from Qian et al. (2018), except for the sources marked with '†' (FIRST survey,
Becker, White & Helfand 1995, White et al. 1997) and '∗' (NVSS, Condon et al. 1998); **Col. 11**: Radio-loudness parameter $R_{1.4\,(\rm GHz)} = flux_{1.4\,(\rm GHz)}\,/\,flux_B$; **Col. 12**: Luminosity at
1.4 GHz, calculated from $flux_{1.4}$ (GHz) (col. 10) and distance d estimated from the distance modulus, i.e. $m_B - M_B = 5\log(d) - 5$.

for each session (online Figs S1–S4). If, however, a PSF gradient was found for a session, no claim of INOV detection was made for that session. We followed this conservative approach in order to ensure that the INOV detections claimed here for our sample of intrinsically weak nearby AGNs are not an artefact due to a gradient in PSF. Figs S1–S4 of the online material show for each session, the differential light curves (DLCs) of the AGNs, relative to two comparably bright steady comparison stars, as well as the 'star1-star2' DLC and the run of PSF through the session. Results for three of the sessions are displayed in Fig. 1. To check for INOV in a session, both DLCs of the AGNs were subjected to the F-test (de Diego 2010; Goyal et al. 2013). Details of the procedure are provided in the online material (Appendix A), together with the methodology for computing the AGN's fractional variability amplitude (ψ) and the DC of INOV for the sample. The DC was computed according to the following definition (Romero, Cellone & Combi 1999):

$$DC = 100\frac{\sum_{\mathbf{i=1}}^{\mathbf{n}} N_i(1/\Delta T_i)}{\sum_{\mathbf{i=1}}^{\mathbf{n}}(1/\Delta T_i)} \text{ per cent} \quad (1)$$

Here, $\Delta T_i = \Delta T_{i,\,\rm obs}(1+z)^{-1}$ is the intrinsic duration of the ith session, obtained by correcting for z of the source ($\Delta T_{i,\,\rm obs}$ is listed in column 4 of the online Table S2). If variability was detected in the ith session, N_i was taken as 1, otherwise $N_i = 0$.

Additional information on the methodology of analysis can be found in Goyal et al. (2013) and Chand et al. (2022). We reiterate that most of the 36 sessions did not witness a systematic drift in PSF (online Figs S1–S4) and all INOV detections claimed here are limited to such sessions only.

4 RESULTS AND DISCUSSION

This study presents the first characterization of INOV for LMAGNs whose BHs have masses tightly clustered around the median value of $10^6 M_\odot$ and all of which have been detected in the X-ray and radio bands. A well-defined representative sample of 12 such LMAGNs (Table 1) was monitored by us in 36 sessions and the resulting DLCs were examined for INOV by applying the F-test (Section 3). Significant INOV was detected in eight sessions (online Table S2) and a mosaic of three of these type 'V' sessions is displayed in Fig. 1. Another two sessions were placed under 'probable variable' (PV) category. All type 'V' sessions showed an INOV amplitude $\psi > 3$ per cent and the corresponding DC of INOV is found to be $\sim$ 22 per cent ($\sim$ 28 per cent, if the two 'PV' type sessions are also included). Here, we recall the extensive INOV study published by Goyal et al. (2013), who followed a very similar analysis procedure and covered six prominent classes of powerful AGNs monitored in 262 sessions, which showed that an INOV amplitude $\psi >$ 3–4 per cent and a DC above $\sim$10 per cent (for $\psi > 3$ per cent) are only observed for blazars [a DC ($\psi > 3$ per cent) $\sim$ 35 per cent was found by them for blazars]. A comparison of these values with the present results reveals a blazar-like level of INOV for the present sample of LMAGNs. It may also be noted that the present estimate of INOV DC ($\psi > 3$ per cent) $\sim$22 per cent for LMAGNs is likely to be an underestimate because the aperture-photometry of these nearby, low-luminosity, AGNs is likely to be significantly contaminated by 'non-variable' emission contributed by the host galaxy, diluting the variable component (e.g. see Ojha et al. 2021). Another potential cause of DC underestimation, as mentioned above, is our conservative approach of restricting claims of INOV to only

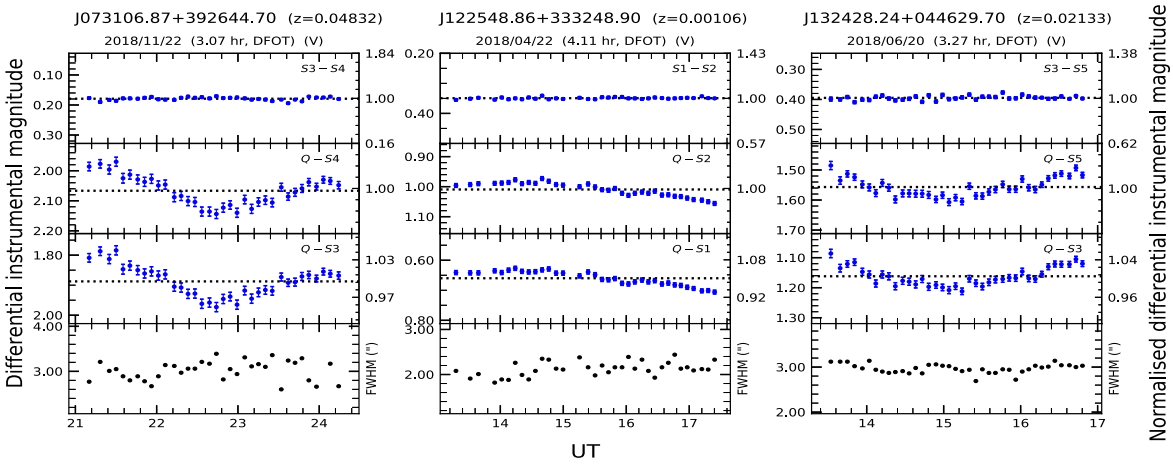

Figure 1. These plots for three out of the total 12 monitoring sessions with INOV detection show DLCs of the AGNs relative to two comparison stars, as well as the star1-star2 DLC (top panel), and the run of the PSF (see the bottom panel for each session). The labels on the right-hand side of each panel show the differential instrumental magnitude normalized by mean value, marked by the dotted horizontal line.

those sessions during which 'seeing' remained steady, i.e. the PSF showed no systematic gradient (online Figs S1–S4).

While the detection of blazar-like INOV levels among the LMAGNs is a pointer to the presence of relativistically beamed jets in them, it is a somewhat unexpected result, on two counts. First, observations indicate that, in comparison to (SMBH powered) blazars, radio-loud NLS1s (including their γ-ray-detected subset) powered by an order-of-magnitude less massive BHs are prone to having only mildly relativistic jets (Angelakis et al. 2015; Gu et al. 2015). Extrapolating this trend to even lower M_{BH} range being probed here, one would expect their jets to be at most mildly relativistic and therefore exhibit only low-level INOV. Secondly, all the 12 LMAGNs monitored here formally belong to the radio-quiet category (Section 2), according to both conventionally adopted criteria, namely, radio luminosity and the radio-loudness parameter (R) (see, however, Ho & Peng 2001). Since powerful RQQs energized by SMBH almost never exhibit a strong INOV with $\psi > 3$–4 per cent (e.g. Gopal-Krishna & Wiita 2018 and references therein), the strong INOV levels found here for the LMAGNs appear striking. However, it may be reiterated that these LMAGNs are not radio-silent and their low radio luminosities are consistent with the non-linear dependence of jet power on M_{BH} ($P_{jet} \propto M_{BH}^{17/12}$, Heinz & Sunyaev 2003; see also Dunlop et al. 2003). Also, their INOV behaviour may be viewed from the perspective of the recent detection of flaring events at 37 GHz in 'radio-silent' NLS1s, occurring several times a year, which has strengthened the case for the capacity of even such radio-silent AGNs to launch relativistic jets (Lähteenmäki et al. 2018). This demonstrates that, at least for moderately massive AGNs, the observed large variability of millimetric flux, probably arising from a relativistic jet, is essentially decoupled from their 'radio-quietness'. It seems reasonable to expect that the optical emission is more closely tied to nuclear jet emission at millimetre wavelengths as compared to its emission at lower frequencies (i.e. radio), which is prone to heavy attenuation due to high opacity on the innermost sub-parsec scales of the nuclear jet, as inferred from VLBI studies (e.g. Gopal-Krishna & Steppe 1991; Boccardi et al. 2017). Conceivably, an extension of the above trend to even less massive AGNs (LMAGNs) being probed here could then explain the strong INOV activity observed in them, despite their being formally 'radio-quiet' (albeit detected in both X-ray and radio bands). Here, it is interesting to recall that for NLS1s, Lister (2018) has underscored the importance of indicators other than radio-loudness, such as flux variability, as proof of relativistic jet.

The present evidence for jet activity in LMAGNs consolidates their usefulness to studies of the 'Fundamental Plane' (FP) of BH activity. This powerful tool, discovered by Merloni, Heinz & di Matteo (2003) and Falcke, Körding & Markoff (2004), has played a prominent role in unifying SMBHs powering AGNs, with solar-mass galactic black holes (GBH) powering X-ray-emitting stellar binaries (see also Falcke & Biermann 1996; Heinz & Sunyaev 2003; Fender, Belloni & Gallo 2004). Basically, FP relates mass accretion rate, proxied by X-ray luminosity, to the jet or outflow power, probed by the radio luminosity, at a given M_{BH}. It is meant to extend the hard-state GBH radio/X-ray correlation (Corbel et al. 2003; Gallo, Fender & Pooley 2003; Maccarone, Gallo & Fender 2003) to include a mass term and thus link the hard-state GBH and their supermassive analogues, altogether spanning ~8 orders of magnitude in M_{BH}. With the evidence for blazar activity, presented here, LMAGNs ($M_{BH} \sim 10^6 M_\odot$) can play a crucial role in defining the FP at the intermediate-mass range. Being 2–3 mag less massive than the SMBH powering blazars, the X-ray segment of their broad-band SEDs would be much less affected by synchrotron cooling, further aided by the spectral Doppler shift pushing the SED to higher energies (e.g. Plotkin et al. 2016; also see Gültekin et al. 2019). These two factors would make the observed X-ray emission of LMAGNs provide a more reliable measure of the mass accretion rate, leading to a more precise determination of the Fundamental Plane.

5 CONCLUSIONS

We have presented the first attempt to characterize INOV of low-mass AGNs (LMAGNs) whose BHs have masses tightly clustered around $10^6 M_\odot$, i.e. near the low-mass end for AGNs and even lower than the mass of the BH at the centre of our galaxy. For this, we monitored in 36 sessions a well-defined representative sample of 12 LMAGNs, each with detected X-ray and radio emission, albeit formally in the radio-quiet domain. The specific question we have addressed is whether such LMAGNs can support nuclear activity, like blazars which are powered by BHs 2–3 orders of magnitudes more massive. The observed similarity of their INOV level to that of blazars hints at the presence of relativistic jets in our set of LMAGNs, akin to the inference reached for 'radio-silent' NLS1 galaxies from their

observed flaring at millimetre wavelengths (Lähteenmäki et al. 2018). It is further noted that such LMAGNs can play an important role in reliable determination of the 'Fundamental Plane' of jet activity in BHs.

ACKNOWLEDGEMENTS

We are thankful to the anonymous referee for constructive suggestions. G-K acknowledges a Senior Scientist fellowship of the Indian National Science Academy. The assistance from the scientific and technical staff of ARIES DFOT and ST is thankfully acknowledged.

DATA AVAILABILITY

The data used in this study will be shared on reasonable request to the corresponding author.

REFERENCES

Abdo A. A. et al., 2009, ApJ, 699, 976
Abolfathi B. et al., 2018, ApJS, 235, 42
Abraham Z., 2000, A&A, 355, 915
Aharonian F. et al., 2007, ApJ, 664, L71
Albert J. et al., 2007, ApJ, 669, 862
Angelakis E. et al., 2015, A&A, 575, A55
Becker R. H., White R. L., Helfand D. J., 1995, ApJ, 450, 559
Begelman M. C., Fabian A. C., Rees M. J., 2008, MNRAS, 384, L19
Blandford R., Meier D., Readhead A., 2019, ARA&A, 57, 467
Boccardi B., Krichbaum T. P., Ros E., Zensus J. A., 2017, A&AR, 25, 4
Britzen S. et al., 2018, MNRAS, 478, 3199
Calafut V., Wiita P. J., 2015, JA&A, 36, 255
Camenzind M., Krockenberger M., 1992, A&A, 255, 59
Cellone S. A., Romero G. E., Combi J. A., 2000, AJ, 119, 1534
Chakrabarti S. K., Wiita P. J., 1993, ApJ, 411, 602
Chand K., Gopal-Krishna, Omar A., Chand H., Mishra S., Bisht P. S., Britzen S., 2022, MNRAS, 511, 13
Condon J. J., Cotton W. D., Greisen E. W., Yin Q. F., Perley R. A., Taylor G. B., Broderick J. J., 1998, AJ, 115, 1693
Corbel S., Nowak M. A., Fender R. P., Tzioumis A. K., Markoff S., 2003, A&A, 400, 1007
de Diego J. A., 2010, AJ, 139, 1269
de Vaucouleurs G., de Vaucouleurs A., Corwin Herold G. J., Buta R. J., Paturel G., Fouque P., 1991, Third Reference Catalogue of Bright galaxies. Springer, New York, NY (USA)
Do T. et al., 2019, ApJ, 882, L27
Dong X.-B., Ho L. C., Yuan W., Wang T.-G., Fan X., Zhou H., Jiang N., 2012, ApJ, 755, 167
Dunlop J. S., McLure R. J., Kukula M. J., Baum S. A., O'Dea C. P., Hughes D. H., 2003, MNRAS, 340, 1095
Falcke H., Biermann P. L., 1996, A&A, 308, 321
Falcke H., Körding E., Markoff S., 2004, A&A, 414, 895
Fender R. P., Belloni T. M., Gallo E., 2004, MNRAS, 355, 1105
Foschini L., 2011, in Foschini L., Colpi M., Gallo L., Grupe D., Komossa S., Leighly K., Mathur S., eds, Proc. Sci., Narrow-Line Seyfert 1 Galaxies and their Place in the Universe. SISSA, Trieste, PoS#24
Foschini L., 2020, Universe, 6, 136
Fuhrmann L. et al., 2016, Res. Astron. Astrophys, 16, 176
Gallo E., Fender R. P., Pooley G. G., 2003, MNRAS, 344, 60
Giannios D., 2010, MNRAS, 408, L46
Giroletti M. et al., 2011, A&A, 528, L11
Gopal-Krishna, Steppe H., 1991, in Miller H. R., Wiita P. J., eds, Variability of Active Galactic Nuclei. Cambridge University Press, Cambridge, England, p. 194
Gopal-Krishna, Wiita P. J., 1992, A&A, 259, 109
Gopal-Krishna, Wiita P. J., 2018, Bull. Soc. R. Sci. Liege, 87, 281
Gopal-Krishna, Stalin C. S., Sagar R., Wiita P. J., 2003, ApJ, 586, L25
Goyal A., Gopal-Krishna, Wiita P. J., Anupama G. C., Sahu D. K., Sagar R., Joshi S., 2012, A&A, 544, A37
Goyal A., Gopal-Krishna, Wiita P. J., Stalin C. S., Sagar R., 2013, MNRAS, 435, 1300
Graham A. W., 2016, in Laurikainen E., Peletier R., Gadotti D., eds, Astrophysics and Space Science Library Vol. 418, Galactic Bulges. Springer-Verlag, Berlin, p. 263
GRAVITY Collaboration, 2018, A&A, 615, L15
Greene J. E., Ho L. C., 2007, ApJ, 670, 92
Greene J. E., Strader J., Ho L. C., 2020, ARA&A, 58, 257
Gu M., Chen Y., Komossa S., Yuan W., Shen Z., Wajima K., Zhou H., Zensus J. A., 2015, ApJS, 221, 3
Gültekin K., King A. L., Cackett E. M., Nyland K., Miller J. M., Di Matteo T., Markoff S., Rupen M. P., 2019, ApJ, 871, 80
Heinz S., Sunyaev R. A., 2003, MNRAS, 343, L59
Ho L. C., Peng C. Y., 2001, ApJ, 555, 650
Jester S. et al., 2005, AJ, 130, 873
Kaspi S., Smith P. S., Netzer H., Maoz D., Jannuzi B. T., Giveon U., 2000, ApJ, 533, 631
Kellermann K. I., Sramek R., Schmidt M., Shaffer D. B., Green R., 1989, AJ, 98, 1195
Kellermann K. I., Condon J. J., Kimball A. E., Perley R. A., Ivezić Ž., 2016, ApJ, 831, 168
Komossa S., 2018, Proc. Sci., Revisiting Narrow-Line Seyfert 1 Galaxies and their Place in the Universe. SISSA, Trieste, PoS#15
Kormendy J., Ho L. C., 2013, ARA&A, 51, 511
Lähteenmäki A., Järvelä E., Ramakrishnan V., Tornikoski M., Tammi J., Vera R. J. C., Chamani W., 2018, A&A, 614, L1
Lister M., 2018, Proc. Sci., Revisiting Narrow-Line Seyfert 1 Galaxies and their Place in the Universe. SISSA, Trieste, PoS#22
Maccarone T. J., Gallo E., Fender R., 2003, MNRAS, 345, L19
Mangalam A. V., Wiita P. J., 1993, ApJ, 406, 420
Marscher A. P., Gear W. K., 1985, ApJ, 298, 114
Marscher A. P., Travis J. P., 1991, NASA STI/Recon Technical Report A, 93, 52913
Merloni A., Heinz S., di Matteo T., 2003, MNRAS, 345, 1057
Mishra S., Gopal-Krishna, Chand H., Chand K., Ojha V., 2019, MNRAS, 489, L42
Nair P. B., Abraham R. G., 2010, ApJS, 186, 427
Nilsson K., Pasanen M., Takalo L. O., Lindfors E., Berdyugin A., Ciprini S., Pforr J., 2007, A&A, 475, 199
Nyland K., Marvil J., Wrobel J. M., Young L. M., Zauderer B. A., 2012, ApJ, 753, 103
Ojha V., Chand H., Krishna G., Mishra S., Chand K., 2020, MNRAS, 493, 3642
Ojha V., Chand H., Gopal-Krishna, 2021, MNRAS, 501, 4110
Paliya V. S., Stalin C. S., Kumar B., Kumar B., Bhatt V. K., Pandey S. B., Yadav R. K. S., 2013, MNRAS, 428, 2450
Paliya V. S., Parker M. L., Jiang J., Fabian A. C., Brenneman L., Ajello M., Hartmann D., 2019, ApJ, 872, 169
Plotkin R. M., Gallo E., Haardt F., Miller B. P., Wood C. J. L., Reines A. E., Wu J., Greene J. E., 2016, ApJ, 825, 139
Qian L., Dong X.-B., Xie F.-G., Liu W., Li D., 2018, ApJ, 860, 134
Romero G. E., Cellone S. A., Combi J. A., 1999, A&AS, 135, 477
Sagar R., 1999, Curr. Sci., 77, 643
Sagar R. et al., 2011, Curr. Sci., 101, 1020
Schmidt M., Green R. F., 1983, ApJ, 269, 352
Seepaul B. S., Pacucci F., Narayan R., 2022, MNRAS, 515, 2110
Spada M., Ghisellini G., Lazzati D., Celotti A., 2001, MNRAS, 325, 1559
Stalin C. S., Gopal Krishna, Sagar R., Wiita P. J., 2004, J. Astrophys. Astron., 25, 1
Stetson P. B., 1987, PASP, 99, 191
Stetson P. B., 1992, in Worrall D. M., Biemesderfer C., Barnes J., eds, ASP Conf. Ser. Vol. Astronomical Data Analysis Software and Systems I. Astron. Soc. Pac., San Francisco, p. 297
Urry C. M., Padovani P., 1995, PASP, 107, 803
Valtaoja E., Terasranta H., Urpo S., Nesterov N. S., Lainela M., Valtonen M., 1992, A&A, 254, 80

Véron-Cetty M. P., Véron P., 2010, A&A, 518, A10
Vestergaard M., Peterson B. M., 2006, ApJ, 641, 689
Wandel A., Peterson B. M., Malkan M. A., 1999, ApJ, 526, 579
White R. L., Becker R. H., Helfand D. J., Gregg M. D., 1997, ApJ, 475, 479
Wilson C. D. et al., 2012, MNRAS, 424, 3050
Witzel G. et al., 2021, ApJ, 917, 73
Yuan W., Zhou H. Y., Komossa S., Dong X. B., Wang T. G., Lu H. L., Bai J. M., 2008, ApJ, 685, 801
Yusef-Zadeh F., Royster M., Wardle M., Cotton W., Kunneriath D., Heywood I., Michail J., 2020, MNRAS, 499, 3909
Zwicky F., Sargent W. L. W., Kowal C. T., 1975, AJ, 80, 545

SUPPORTING INFORMATION

Supplementary data are available at *MNRASL* online.

Figure S1. Differential light curves (DLCs) for our sample of 12 low-mass, radio/X-ray-detected AGNs.

Figure S2. Same as Fig. 1.
Figure S3. Same as Fig. 1.
Figure S4. Same as Fig. 1.
Table S1. Basic parameters of selected pool of comparison stars.
Table S2. Result of the statistical test for detecting INOV in the DLCs of the 12 LMAGNs (taking $\eta = 1.54$, see Appendix A).

Please note: Oxford University Press is not responsible for the content or functionality of any supporting materials supplied by the authors. Any queries (other than missing material) should be directed to the corresponding author for the article.

This paper has been typeset from a TEX/LATEX file prepared by the author.